Available online at www.sciencedirect.com
ScienceDirect
Journal of Nuclear Materials 367–370 (2007) 191–195
journal of nuclear materials
www.elsevier.com/locate/jnucmat

Effect of milling on morphological and microstructural properties of powder particles for High-Cr Oxide dispersion strengthened ferritic steels

Noriyuki Y. Iwata [a,*], Akihiko Kimura [a], Masayuki Fujiwara [b], Norimichi Kawashima [c]

[a] *Institute of Advanced Energy, Kyoto University, Gokasho, Uji, Kyoto 611-0011, Japan*
[b] *Kobelco Research Institute Inc., Takatsukadai 1-5-5, Nishi-ku, Kobe 651-2271, Japan*
[c] *Toin University of Yokohama, Kurogane 1614, Aoba-ku, Yokohama 225-8502, Japan*

Abstract

The morphological and microstructural properties of powder particles were examined systematically to optimize the milling time for producing high-chromium oxide dispersion strengthened (ODS) ferritic steels. The XRD and SEM results showed that peak broadening in the XRD patterns occurred due to a decrease in the grain size and the particle diameter of the powder during mechanical milling. The particle size distribution range decreased first with increasing the milling time up to 12 h and then clearly increased thereafter. After 12 h milling, the particles were nearly spherical with nearly uniform mean size of 5.9 μm. SEM–EDS analysis of the particle surface showed all distributed homogeneously.

1. Introduction

Oxide dispersion strengthened (ODS) ferritic steels have been developed for application as fast breeder reactor (FBR) fuel cladding materials because of their excellent high-temperature strength and radiation resistance [1,2]. In particular, ODS ferritic steels with chromium (Cr) concentration of 14–22 wt% have superior corrosion resistance in super critical pressurized water (SCPW) [3,4]. Thus, the ODS ferritic steels are also considered to be a candidate material for water-cooled fusion systems.

The application of the ODS ferritic steels in fusion blankets is essential for increasing thermal efficiency of the blanket system. The material properties required for the advanced fusion blanket systems are: (i) high-temperature strength, (ii) high resistance to irradiation embrittlement and swelling, (iii) compatibility with coolant at high temperatures, and (iv) low susceptibility to hydrogen-induced cracking and stress corrosion cracking (SCC).

Performance of the ODS ferritic steels depend on the nano-scale oxide particle dispersion states,

* Corresponding author. Tel.: +81 774 38 3478; fax: +81 774 38 3479.
E-mail address: noriyuki76@iae.kyoto-u.ac.jp (N.Y. Iwata).

0022-3115/$ - see front matter © 2007 Elsevier B.V. All rights reserved.
doi:10.1016/j.jnucmat.2007.03.147

including size, number density, microstructure, and chemical composition. High-density dispersions of nano-sized oxide particles are indispensable to enhance high-temperature strength [5–9]. The technique of dispersing oxide particles into the matrix of the ODS ferritic steels is critical to achieving good material performance, and it is expected that the dispersion condition is influenced strongly by the properties of raw material powders both before and after mechanical alloying (MA).

The goal of the present study is to establish the optimized powder processing to enhance the performance of the ODS ferritic steels. In this work, the effect of milling on the morphological and microstructural properties of powder particles was examined systematically by optimizing milling time to improve the powder processing of ODS steels production.

2. Experimental

2.1. Powder preparation

Elemental powders of aluminum (Al), chromium (Cr), iron (Fe), titanium (Ti), tungsten (W), and yttria (Y_2O_3) were weighted separately in a pure argon atmosphere and mixed to give the desired composition, Fe–16Cr–4Al–0.3Ti–1.8W–0.35Y_2O_3. The mixed powder was sealed in a grinding container with Fe–12Cr–2.1C–0.3Si–0.3Mn balls. Mechanical alloying (MA) was conducted on a planetary ball mill (Pulverisette-5, Fritsch GmbH, Germany) at room temperature for various times. A ball-to-powder weight ratio of 15:1 and a rotational speed of 180 rpm were adopted for performing this study.

2.2. Characterization

The crystal structure of the powder was examined by X-ray diffractometer (XRD; RINT-2000, Rigaku Co., Japan) with Cu Kα radiation. The particle size distribution was measured by means of a laser diffraction scattering method using a particle size analyzer (LS-230, Beckman Coulter Inc., Japan). The surface morphology was observed using a scanning electron microscope (SEM; JSM-5310, JEOL Ltd., Japan). The element distribution and composition were analyzed by using the energy dispersive spectroscopy (EDS; JED-2140, JEOL Ltd., Japan) equipment on the SEM instrument.

3. Results and discussion

3.1. Influence of milling on crystal structure

The structure of the powder was first examined by powder X-ray diffraction (XRD). Fig. 1 shows the XRD spectra of the mixed powder before and after milling for the indicated time periods. The milling time sequence runs from the top to the bottom of the figure. In comparison with JCPDS data card, the main diffraction peaks can be well indexed to aluminum (Al), tungsten (W), and iron (Fe). A decrease in the diffraction peak intensity was clearly observed with increased milling time. Although the peak intensities of Al and W decreased remarkably at the early stage of milling as compared with that of Fe, a drastic decrease in the peak intensity for W (1 1 0) was less intense than that for Al (1 1 1). The diffraction peak width of the overlapping Fe (1 1 0) and Cr (1 1 0) appears to be independent of the milling time.

These results show that it is difficult to reduce the particle size of ductile Fe powder, even with high energy input mechanical alloying (MA). On the other hand, all the diffraction peaks except for Fe (1 1 0) became indistinct and broader with increasing milling time. The peak broadening detected in the patterns suggests that both the particle diameter and also grain size of the mixed powder were effectively decreased by the mechanical milling.

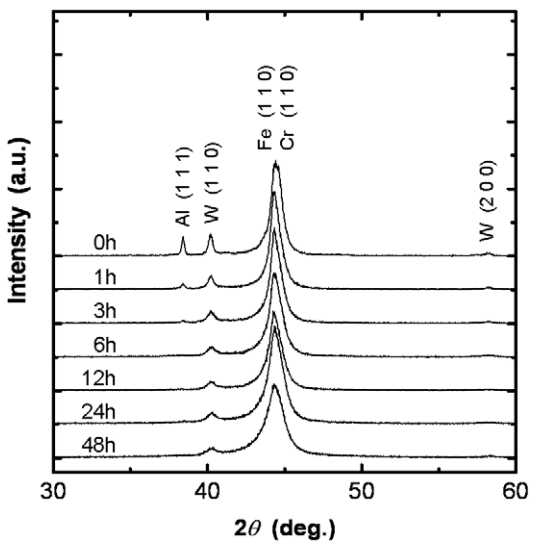

Fig. 1. XRD spectra of the mixed powder before and after milling for the indicated time periods.

The XRD patterns show clearly that the powder processed by MA reduces the diffraction peak intensity. On the basis of the XRD measurement results, the grain size, D, is defined by the following Scherrer equation:

$$D = \frac{0.9\lambda}{\beta \cos\theta}, \quad (1)$$

where λ, β, and θ are the X-ray wavelength, full width at the half-maximum (FWHM) of the peak for W (1 1 0) shown in Fig. 1, and diffraction angle, respectively. Fig. 2 shows the grain size of the mixed powder as a function of the milling time. The grain size decreased from 40 to 21 nm with increasing milling time to 12 h and then leveled off thereafter. The saturation occurs at around 12 h.

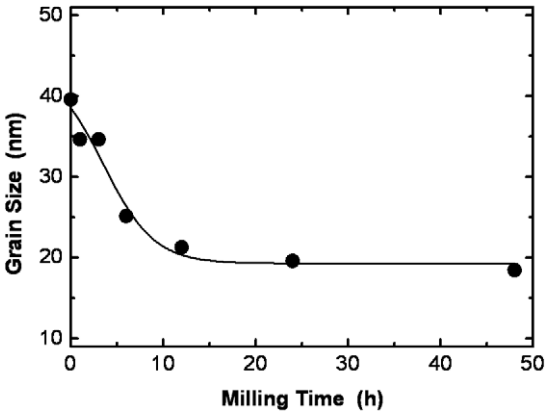

Fig. 2. Grain size in the mixed powder as a function of the milling time.

3.2. Influence of milling on particle size distribution and morphology

In order to characterize the powder before and after the MA, the particle size distribution was measured using a particle size analyzer. Fig. 3 shows the particle size distributions of the mixed powder (a) before milling, and after milling for (b) 1, (c) 6, (d) 12, (e) 24, and (f) 48 h. The size distribution of the powder before milling can be fit by four distributed peaks with average particle diameters of approximately 3, 7, 15, and 30 μm. The distribution peaks of the coarse particles shifted gradually toward smaller values and clearly narrowed with increased milling time. After 12 h milling, the distribution separated into four peaks with average diameters of about 3, 7, 14, and 25 μm. In contrast, the particle diameter and size distribution range increased thereafter with additional mechanical milling.

In our previous work, we systematically investigated each raw material powder, i.e., commercial metal and/or oxide powder particles, for production of the oxide dispersion strengthened (ODS) ferritic steels. We found that the average particle diameter of Fe powder was 4.3 μm [10]. That result is consistent with the present measurements for the mixed powders shown in the figure, with the minimum

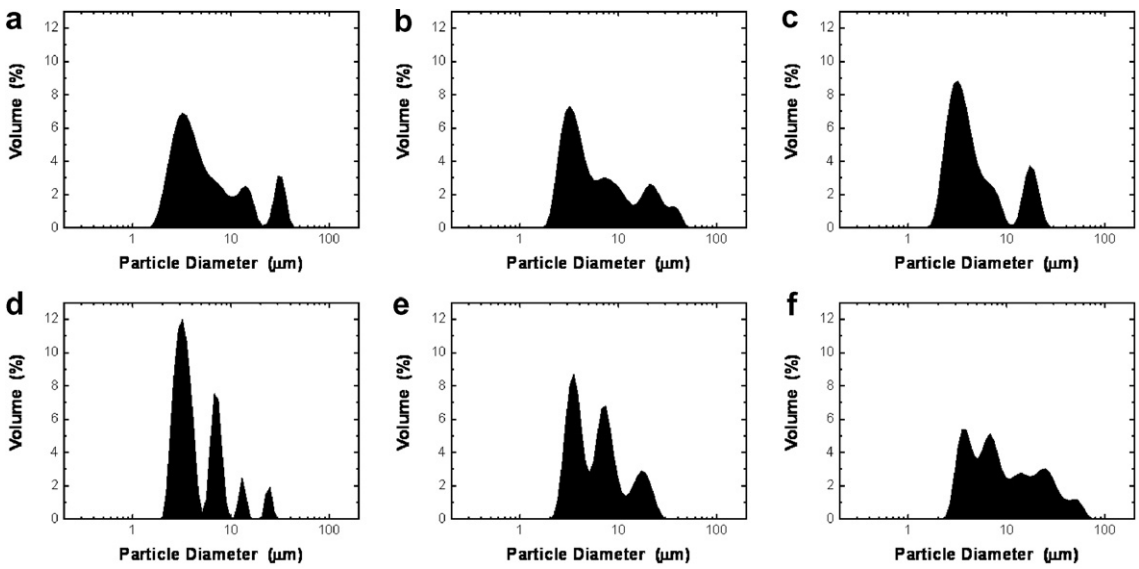

Fig. 3. Particle size distributions of the mixed powder (a) before and after milling for (b) 1, (c) 6, (d) 12, (e) 24, and (f) 48 h.

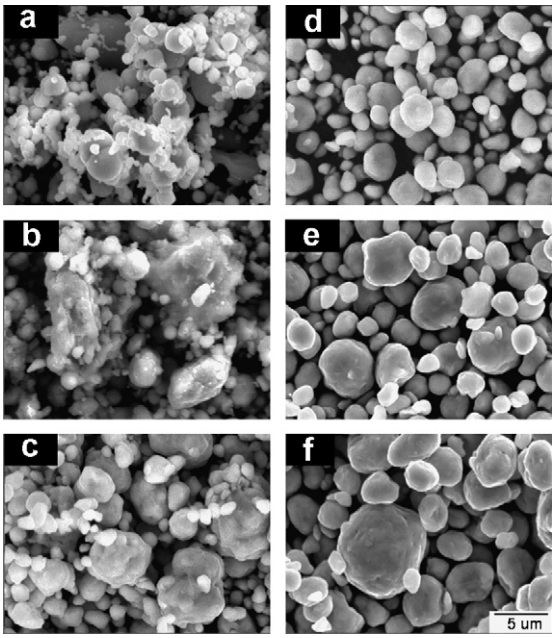

Fig. 4. SEM images of the mixed powder (a) before and after milling for (b) 1, (c) 6, (d) 12, (e) 24, and (f) 48 h.

distribution peak of each powder particle consistently near 3 μm diameter. This indicates that the milling ability depends on the starting raw material powder.

Typical SEM images of the mixed powder (a) before, and after milling for (b) 1, (c) 6, (d) 12, (e) 24, and (f) 48 h are shown in Fig. 4. The powder before milling is composed of irregular agglomerated particles, which means that sub-micrometer particles with various shape condense into several-μm-size particles with approximately spherical shape. The particle size increased slightly through the primary particle agglomeration into larger secondary particles after 1 h milling and then clearly decreased on increasing the milling time. It is noted here that an increase in the size occurred at the early stage of milling. Beyond 1 h milling, the high energy input by MA induced a decrease of the particle size, because the particle diameter became distinctly larger than that before milling. After 12 h milling, the micrograph shows that the mixed powder were more closely spherical in shape with a more uniform averaged size. In contrast, the particle size increased at a slow rate thereafter with additional mechanical milling. These results are in good agreement with the particle size distributions in Fig. 3.

The particle size of the powder was also calculated automatically in the former particle size distribution measurement. Fig. 5 exhibits the mean particle size of the mixed powder as a function of the milling time. The particle size decreased first gradually with increasing milling time up to 12 h and then increased drastically thereafter with further milling. The minimum value of the mean particle size is 5.9 μm, observed at 12 h milling.

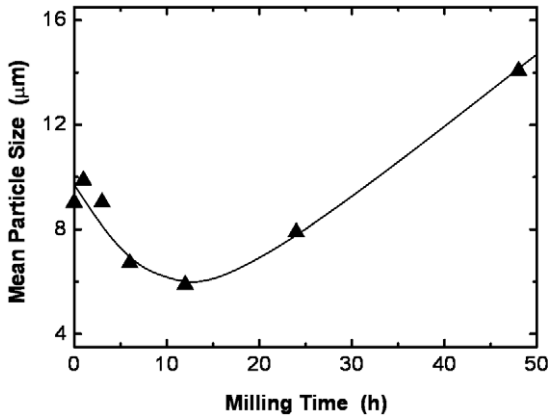

Fig. 5. Mean particle size of the mixed powder as a function of the milling time.

3.3. Element distribution and chemical composition

The element distribution and composition of the powder were analyzed by the energy dispersive

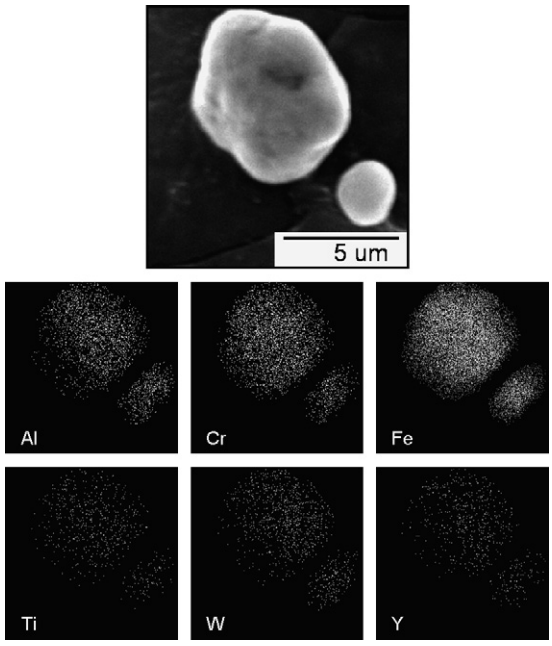

Fig. 6. SEM–EDS results on composition of the mixed powder after milling for 12 h.

Table 1
Chemical compositions of the mixed powder before and after milling for 12 h

Milling time (h)	Chemical composition (wt%)							
	C	Al	Cr	Fe	Ti	W	Y_2O_3	Ex.O
0	–	4.00	16.00	Bal.	0.30	1.80	0.35	–
12	0.04	4.05	16.08	Bal.	0.39	1.17	0.37	0.05

spectroscopy (EDS) system on the SEM instrument. Fig. 6 shows the SEM–EDS results of the mixed powder after milling for 12 h. The SEM image and element distribution maps show that all the elements provided as raw material powder are distributed homogeneously on the particle surface. The chemical compositions of the mixed powder before and after milling for 12 h are also shown in Table 1. As can be seen in the table, there is no great compositional difference between the particle surface before and after milling, even for the particles processed at 12 h milling. The exception is some segregation of W.

4. Summary

The morphological and microstructural properties of powder particles were systematically examined to control the powder processing of high-chromium oxide dispersion strengthened (ODS) ferritic steels. The results obtained are summarized as follows:

1. Although the grain size and particle diameter of the mixed powder was effectively decreased by mechanical milling, it is difficult to reduce the particle size of ductile Fe powder, even with high energy input mechanical alloying (MA).
2. The particle size and size distribution range decreased gradually with increasing milling time up to 12 h and then increased drastically thereafter. This indicates that the limits of milling depend on the raw material powder, i.e., starting metal and/or oxide powder particles.
3. The powder before milling is composed of submicrometer particles with various shape. These agglomerate into several micrometer particles with near-spherical shape. After 12 h milling, the particle shape became more closely spherical with more uniform size and mean particle size of 5.9 μm.
4. All elements provided in the raw material powder distribute homogeneously on the particle surface, with no great difference in the chemical compositions detected before and after milling, even for the particles processed by 12 h milling.

Thus, there is an optimum milling time for manufacturing mixed powder from starting raw-powder particles for high-Cr ODS ferritic steels production. Optimum milling provides the smallest particle size and uniform chemical composition.

Acknowledgment

This work was partly supported by a 21st Century Center of Excellence (COE) Program Grant from the Ministry of Education, Culture, and Sports, Science and Technology of Japan.

References

[1] S. Ukai, T. Nishida, H. Okada, T. Okuda, M. Fujiwara, K. Asabe, J. Nucl. Sci. Technol. 34 (1997) 256.
[2] S. Ukai, T. Nishida, T. Okuda, T. Yoshitake, J. Nucl. Sci. Technol. 35 (1998) 294.
[3] A. Kimura, S. Ukai, M. Fujiwara, in: Proceedings of the 2004 International Congress on Advances in Nuclear Power Plants (ICAPP '04), CD-ROM, 2004, Paper 2070.
[4] H.S. Cho, A. Kimura, S. Ukai, M. Fujiwara, J. Nucl. Mater. 329–333 (2004) 387.
[5] R.W. Evans, J. Preston, B. Wilshire, E.A. Little, J. Nucl. Mater. 195 (1992) 24.
[6] S. Ukai, M. Harada, H. Okada, M. Inoue, S. Nomura, S. Shikakura, K. Asabe, T. Nishida, M. Fujiwara, J. Nucl. Mater. 204 (1993) 65.
[7] D.K. Mukhopadhyay, F.H. Froes, D.S. Gelles, J. Nucl. Mater. 258–263 (1998) 1209.
[8] S. Ukai, T. Nishida, T. Okuda, T. Yoshitake, J. Nucl. Mater. 258–263 (1998) 1745.
[9] I.S. Kim, J.D. Hunn, N. Hashimoto, D.L. Larson, P.J. Maziasz, K. Miyahara, E.H. Lee, J. Nucl. Mater. 280 (2000) 264.
[10] N.Y. Iwata, A. Kimura, S. Ukai, M. Fujiwara, N. Kawashima, in: Proceedings of the 2005 International Congress on Advances in Nuclear Power Plants (ICAPP '05), CD-ROM, 2005, Paper 5528.